

Available online at www.sciencedirect.com

Energy Procedia 6 (2011) 46–54

Energy

Procedia*MEDGREEN 2011-LB*

Hydrogen production over $\text{CuIn}_3\text{Se}_5/\text{WO}_3$ hetero-junction

Lyakout Djellal^{a*}, Bachir Bellal^b, Mohammed Trari^b

^a *Laboratoire des Solutions Solides, Faculté de Physique. E-mail adress : dlyakout@hotmail.com* ^b *Laboratoire de Stockage et de Valorisation des Energies Renouvelables, Faculté de Chimie, (USTHB) BP 32 El Alia 16111, Algiers, Algeria.*

Abstract

The hydrogen photo-evolution was successfully achieved over $\text{CuIn}_3\text{Se}_5/\text{WO}_3$ hetero-junction. CuIn_3Se_5 powder has been synthesized by fusion technique. The compound crystallizes in the chalcopyrite structure and exhibits *n*-type conductivity. The optical gap (1.19 eV) was determined from the reflectance diffuse spectrum and the flat band potential (-0.22 V) from the Mott Schottky plot. The small forbidden band and the negative flat band potential make it promising for the solar energy conversion.

In aqueous solutions, the material is stabilized by hole consumption involving X^{2-} species ($= \text{S}^{2-}$ and $\text{S}_2\text{O}_3^{2-}$). H_2 formation would become thermodynamically easy in alkaline media. The best performance was obtained in $\text{S}_2\text{O}_3^{2-}$ solution (10^{-2} M, pH~7) with an evolution rate of $0.54 \text{ mL g}^{-1} \text{ min}^{-1}$. The photo activity is ascribed to electrons transfer from the sensitizer CuIn_3Se_5 -Conduction Band (CB), acting as electrons pump, to WO_3 -CB (-0.4 V_{VS} SCE) resulting in the enhanced water reduction.

© 2010 Published by Elsevier Ltd. Open access under [CC BY-NC-ND license](http://creativecommons.org/licenses/by-nc-nd/3.0/).
Selection and/or peer-review under responsibility of [name organizer]

Keywords: Hydrogen; Chalcopyrite; CuIn_3Se_5 ; Hetero-junction

* Corresponding author. Tel.: +0-213-021-247-344; fax: +0-213-021-247-344.
E-mail address: dlyakout@hotmail.com

1. Introduction

The photo-electrochemical (PEC) conversion of light-to-chemical energy continues to attract much attention owing to the depletion of fossil energies and ecological problems [1-3]. A great attention has been focused upon hydrogen as a clean energetic vector. It is predictable to be the energy of the future which should reduce greenhouse emission, responsible of the climate change. Water decomposition is one of the most attractive processes to get pure hydrogen. For efficient PEC device, n-type SC requires not only a small gap and a long term chemical stability but also a flat band potential (V_{fb}) as cathodic as possible. The search of photo-active materials with small optical gap led us to study chalcopyrite semiconductors. For these semiconductors, conduction band lies at a potential not negative enough to liberate hydrogen with appreciable rates. This can be surmounted by using materials whose electronic bands derive from less electronegative elements and pH insensitive like materials belonging to the ternary system Cu-In-Se [4]. $CuIn_3Se_5$ is predicted to be a good sensitizer. More recently, we reported the feasibility of $CuInSe_2$ for hydrogen- production upon visible light [5]. In the present work, we extend the work to $CuIn_3Se_5$ and $CuIn_3Se_5/WO_3$ hetero-system.

2. Experimental method

Ingots of $CuIn_3Se_5$ were synthesized by the melt technique, the procedure was described in details elsewhere [6]. The phase has been identified by X-ray diffraction (XRD) using $Cu K_{\alpha}$ radiation ($\lambda = 0.154178$ nm). The chemical composition was carried out by the energy dispersive spectroscopy (EDS) at accelerating voltages of 25 kV using an ESEM XC 30 FEC. The powder was characterized by the diffuse reflectance spectrum with a Cary 500 Varian double beam spectrophotometer and MgO-coated integrating-sphere reflectance attachment. The electrical conductivity (σ) was measured by the two probe method in the temperature range (300-870 K). Ohmic contact with copper wire was made with silver cement on the slices which were encapsulated in glass holders with epoxy resin to form the working electrodes. For PEC characterization, a three electrode cell was employed including the working electrode, the emergency Pt counter electrode (Tacussel) and the saturated calomel electrode (SCE). The working electrode was irradiated by a tungsten lamp (200 W) and the potentials were monitored by a Voltalab PGZ301 potentiostat (Radiometer). The electrolyte KOH (0.1 M) was continuously flushed with nitrogen and the experiments were performed at room temperature. The intensity-potential $J(V)$ curves and the capacitance measurements were plotted by a Voltalab potentiostat PGP 301. A response analyzer was used to generate 10 mV perturbing signals with frequencies ranging from 1 mHz to 100 kHz and subject the electrode to various potentials. The photocurrent-photovoltage (J_{ph} - U_{ph}) plots were recorded in a two electrode cell with external resistance boxes and two multimeters.

The photocatalytic experiments were carried out in a closed gas circulation equipped with a double wall cylindrical Pyrex reactor. The temperature of the solution was kept at $(50 \pm 1$ °C) thanks to a thermo stated bath. The powder was dispersed under constant magnetic agitation. Visible light, produced by three tungsten lamps, was used as excitation source. Before each run, the solution was desaturated in advance for 35 min by nitrogen. Blank runs were carried out without the catalyst and in the dark. The outgoing gas has been positively identified as hydrogen by gas chromatography (Shimadzu IGC121 ML) and the amount was determined volumetrically thanks to a water manometer. The solutions were prepared from reagents of analytical quality and twice distilled water. WO_3 was purchased from Merck and used without any further treatment.

3. Results and discussion

The elaborated CuIn_3Se_5 crystallizes in the chalcopyrite structure (space group: $\bar{P}4_2c$) (Fig. 1). The lattice constants $a = 0.5740$ nm and $c = 1.1501$ nm, refined by the least square method agree with those reported previously [7, 8]. The crystallite size D (32 nm) was estimated through the relation $\{D = 0.94\lambda/\beta \cos \theta\}$, θ being the diffraction angle.

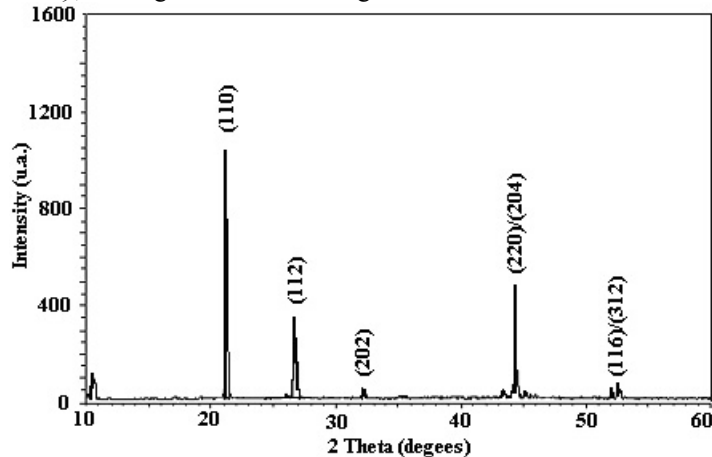


Fig. 1 X-ray diffraction pattern of CuIn_3Se_5 powder elaborated from stoichiometric melt

The EDS spectrum gives an average atomic composition (Cu= 11.05 at.%, In= 33.55 at.%, Se= 55.40 at.%), fairly close to the stoichiometric formulation CuIn_3Se_5 with however a slight indium excess.

The optical gap (E_g) was determined from the diffuse reflectance spectrum (Fig. 2). The linear plot of the absorption coefficient (α) on the photon energy: $(\alpha h\nu) \sim (h\nu - E_g)^{1/2}$ gives a gap E_g of 1.19 eV close to that reported the literature [9].

The transport properties are enhanced by deviation from the stoichiometry. The n-type conductivity of CuIn_3Se_5 is due to associated with In excess. The increase of the conductivity (σ) with temperature indicates semi conducting-like behavior (inst, Fig. 2) which obeys to an Arrhenius type law ($\sigma = \sigma_0 \exp(-\Delta E_\sigma/kT)$) where σ_0 being the pre exponential term. From the plot $\log \sigma$ vs. $1000/T$, the large activation energy ($\Delta E_\sigma = 0.52$ eV), calculated from the straight line in the heating direction, ($\sim E_g/2$) indicates that CuIn_3Se_5 approaches intrinsic conductivity where nearly all the donors are bonded at room temperature with a Fermi level E_f located in the middle of the forbidden band.

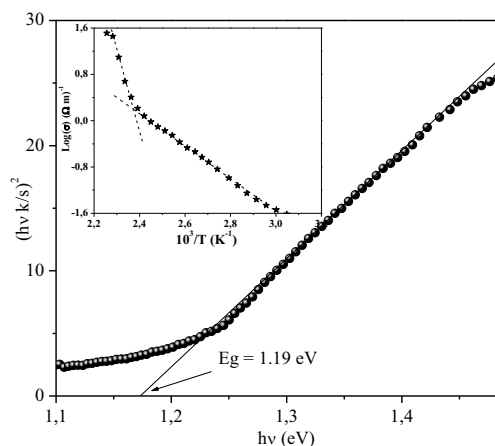


Fig. 2 The plot $(k/s \cdot hv)^2$ versus $h\nu$ of $CuIn_3Se_5$. Insert: $\text{Log}(\sigma)$ versus reciprocal temperature

The photo-electrochemistry provides information about the energy band diagram of the interface semiconductor (SC)/electrolyte and enables the prevision of electrochemical reactions. The chemical inertness is a crucial parameter for a reliable catalytic performance. $CuIn_3Se_5$ exhibits a good chemical stability over the whole pH range. The chemical stability is attributed to the fact that the electronic states of the highest VB in which the reacting holes are generated are mainly formed from hybridized Se: $4s\text{-Cu}$: $3d$ orbitals [10]. The corrosion rate in KCl (0.5 M), calculated from titrated copper by iodometry, was found to be $1.2 \mu\text{mol m}^{-2} \text{year}^{-1}$. Such value is corroborated by the semi logarithmic plots ($\log J\text{-V}$) (inst, Fig.3) where a corrosion potential of 0.1 V, an exchange current density J_0 of $1.2 \mu\text{A cm}^{-2}$ and a polarization resistance of $200 \Omega \text{cm}^{-2}$ were determined.

The $J(V)$ curve (Fig. 3) exhibits a dark current (J_d) smaller than $50 \mu\text{A cm}^{-2}$, in conformity with a good electrochemical stability. The potential at which the $J_d\text{-V}$ curve intercepts the potential-axis corresponds to the hydrogen evolution reaction. The increase of the photo-current (J_{ph}) along the anodic-going polarization is characteristic of n-type conductivity.

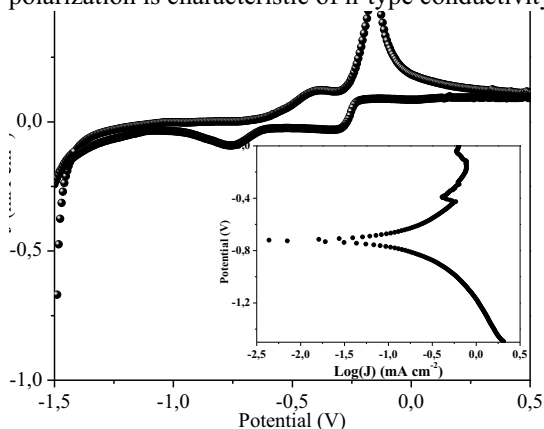


Fig. 3 The cyclic $J(V)$ curve of $CuIn_3Se_5$ in the dark. Electrolyte KOH (0.5 M), scan rate 10 mVs^{-1} Insert: The Semi logarithmic plot of $CuIn_3Se_5$ in KCl (0.5 M).

The accurate flat band potential V_{fb} is obtained from the Mott Schottky plot (Fig. 4):

$$C^{-2} = 2(\epsilon\epsilon_0 e N_d)^{-1} (V - V_{fb})$$

where all the symbols have their usual significations. By extrapolating the plot to $C^{-2} = 0$, the potential V_{fb} was found to be -0.22 V. The positive slope confirms once again the n type conductivity and gives a donor density N_D equal to $3.75 \times 10^{16} \text{ cm}^{-3}$. The bending observed for positive potentials is attributed to a neglected recombination rate of electron/hole (e^-/h^+) pairs i.e. further away from V_{fb} and indicates a charge accumulation near the interface with a high series resistance. The permittivity ϵ ($= 10$) has been determined independently from the dielectric measurement.

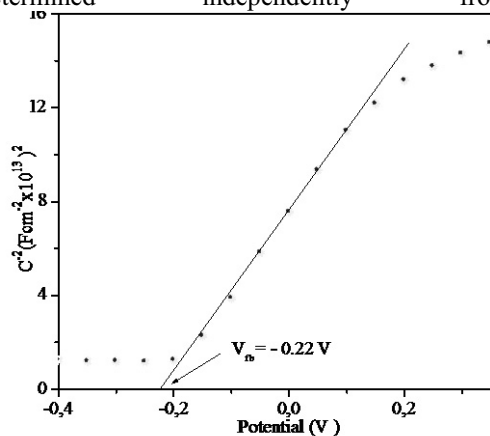


Fig. 4 The Mott-Schottky plot for $n\text{-CuIn}_3\text{Se}_5$. The frequency was set at $2 \times 10^4 \text{ s}^{-1}$ in KOH (0.5 M), scan rate 10 mV s^{-1}

The energy of VB is given by :

$$P = e V_{fb} - \Delta E_{\sigma} + 4.75$$

4.75 represents the free energy of the electrode (SCE) relative to vacuum. The calculated P value (5.47 eV) is typical of materials in which VB is made up mainly from Se: $4p$ orbital with little admixture of Cu: $3d$ in agreement with the results of ref. [10]. CB is positioned at 4.01 eV below vacuum, typical for materials in which CB is made predominantly by indium orbital.

The above characterizations (transport properties and photo electrochemistry) allow the establishment of the energy band diagram (Fig.5). From a thermodynamic point of view, spontaneous H_2 evolution under visible light is predicted. $\text{CuIn}_3\text{Se}_5\text{-CB}$ is positioned at -0.74 V and therefore lies below the $\text{H}_2\text{O}/\text{H}_2$ (-0.6 V), determined from the $J(V)$ characteristic.

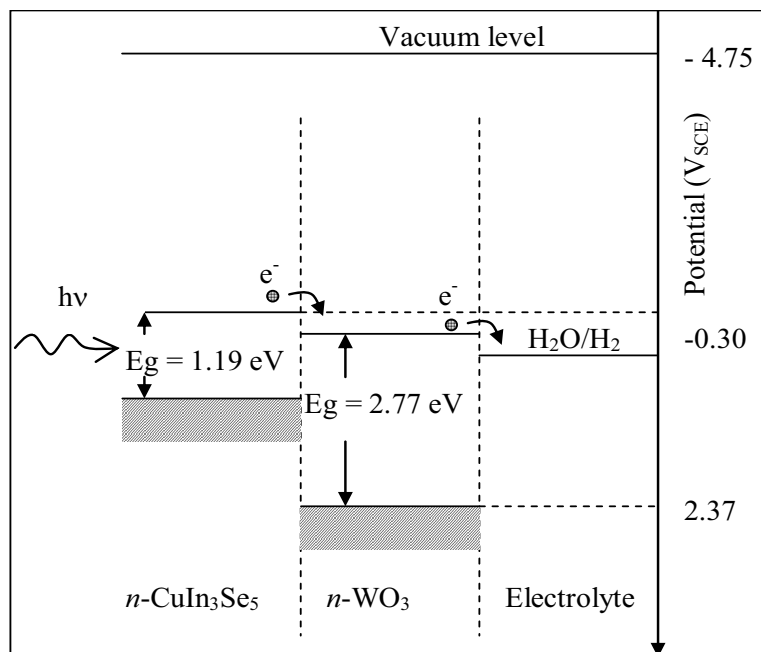


Fig. 5 The energy band diagram of the system $n\text{-CuIn}_3\text{Se}_5/n\text{-WO}_3/\text{KOH}$ electrolyte

The light absorption induces a charge separation of the (e^-/h^+) pairs within the diffusion length and the PEC process is restricted to a micro reaction space. Both half electrochemical reactions occur simultaneously on a single crystallite that works like a micro PEC cell. In order to collect most photoelectrons, an anodic voltage must be applied to CuIn_3Se_5 which generates a space charge region (SCR) at the interface. The degree the band bending (B) is expected to be less in the crystallite than can be induced in SC electrode and the separation of (e^-/h^+) pairs should be less efficient in powder and the recombination of (e^-/h^+) pairs depends on the B-value. However, the potential V_{fb} should give rise to a large bending at the interface $\text{CuIn}_3\text{Se}_5/\text{electrolyte}$ in presence of negative redox couple. Moreover, the PEC process may be kinetically enhanced in presence of reducing agent which competes with the photodissolution and stabilize CuIn_3Se_5 ; thiosulfate $\text{S}_2\text{O}_3^{2-}$ being particularly favorable. It is helpful to outline that only redox couples having $E_{red}^\circ > E_{decom}^\circ$ should be used keeping in mind that E_{red} does not exceed VB. Otherwise the holes cannot protect the material against the photocorrosion. For the crystallite, the width of SCR is given by:

$$W = \{2 \varepsilon \varepsilon_0 (E_{red} - V_{fb}) / e N_a\}^{0.5}$$

A further condition to eventuate in photoreductions is that the free potential U_f of $n\text{-CuIn}_3\text{Se}_5$ must be positive of the potential V_{fb} . The maximal width W (230 nm) is obtained in $\text{S}_2\text{O}_3^{2-}$ solution ($E_{red} - V_{fb} = 0.22$ V). In addition, the potential U_f (~ 0 V) indicates that the crystallite is protected cathodically against the corrosion according to the potential-pH diagram of the system Cu-In-Se [11]. As noticed above, V_{fb} does not vary significantly with pH and one would have the further advantage to move adequately the $\text{H}_2\text{O}/\text{H}_2$ level with respect to CB by changing the pH. This hypothesis has been tested successfully with $\text{S}_2\text{O}_3^{2-}$ and S^{2-} . For both species X^{2-} , the volume of hydrogen increases linearly with irradiation time and tends to saturation after ~ 10 mn (Fig. 6). This tendency to saturation is due to the reduction of the end products which take place in competition with the hydrogen evolution.

The greater volume of evolved H_2 with $S_2O_3^{2-}$ is easily understood in terms of the kinetic parameters since the band bending ($\Delta\Phi$) at the interface i.e. the driving force is nearly the same for both couples $SO_3^{2-}/S_2O_3^{2-}$ (0.46) and S_n^{2-}/S^{2-} (0.41).

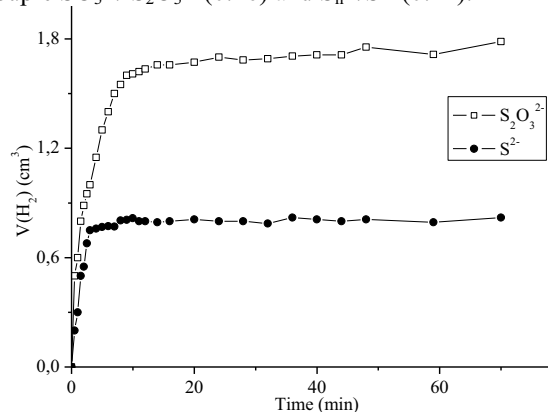


Fig. 6 Volume of evolved H_2 versus illumination time over $CuIn_3Se_5$ in $S_2O_3^{2-}$ and S^{2-}

The quantum yield (η) of the light conversion into hydrogen is given by:

$$\eta = 2 \{ \text{number of } H_2 \text{ mol. sec}^{-1} / \text{photons flux sec}^{-1} \}$$

The factor 2 enters in the relation because the hydrogen evolution is two electrons event. A value of 0.13 % has been found under polychromatic light. According to the Gartner model, the variation of η is given by:

$$-\ln(1 - \eta) = \alpha \{ 2\epsilon\epsilon_0/eN_D \}^{1/2} (V - V_{fb})^{1/2} + \ln(1 - \alpha L)$$

The equation is valid away from the potential V_{fb} i.e. the recombination process is low. From the linear relation between $-\ln(1-\eta)$ vs. $(V - V_{fb})^{1/2}$, α and L (table 1) have been determined respectively from the slope and the intercept of the linear plot. The depletion width W is larger than both the diffusion length L (except for 620 nm) and the crystallite size D and this indicates that practically all the pairs (e^-/h^+) generated within the length W are collected efficiently and contribute to the H_2 evolution.

Individually, CIS_{35} is less active compared to $CuInSe_2$ [5] and some attempts have been made to improve its photocatalytic performance. A particular attention would be therefore directed towards the hetero-system CIS_{35}/WO_3 . The enhancement is attributed to the electron transfer from CB of activated $CuIn_3Se_5$ to WO_3 -CB resulting in the reduction of H_2O into hydrogen. The selected material WO_3 is chemically stable in neutral medium and exhibits n type conduction attributed to oxygen vacancies. However, it shows a poor photocatalytic hydrogen evolution. With a gap of 2.7 eV, most of the sun spectrum is sub band gap and therefore weakly converted. Both the electronic bands of WO_3 and the potential of H_2O/H_2 couple vary by ~ -0.06 V/pH in contrast to $CuIn_3Se_5$. $CuIn_3Se_5$ works as electrons pump and the electron transfer is due to the efficient charge separation because the energy difference between the two semiconductors which increases with decreasing pH; this prevents the reverse flow and in this way the lost of the (e^-h^+) pairs by recombination process. At pH 7, the photoelectrons in $CuIn_3Se_5$ -CB (-0.74 V) are transferred to WO_3 -CB (-0.4 V) itself more negative than the H_2O/H_2 potential to reduce spontaneously water into hydrogen. The noticeable enhancement is partially attributed to intimate contact between WO_3 and $CuIn_3Se_5$ which enables a transfer of excited photoelectrons. Conceivably, the hydrogen evolution proceeds mostly on WO_3 while the oxidation of $S_2O_3^{2-}$ ($2 S_2O_3^{2-} + 2 h^+ \rightarrow S_4O_6^{2-}$) occurs over $CuIn_3Se_5$ (Fig. 7). Over time, the hydrogen tends toward saturation. The competitive reduction of $S_4O_6^{2-}$ is therefore thought to be the main reason for the curvature $V(H_2)$ -time.

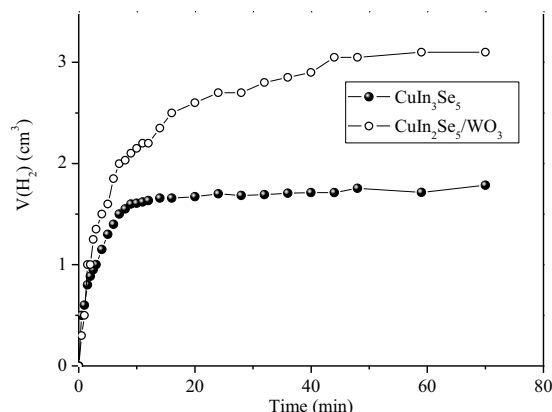


Fig. 7 Volume of evolved H_2 versus illumination time over CuIn_3Se_5 and $\text{CuIn}_3\text{Se}_5/\text{WO}_3$ in $\text{S}_2\text{O}_3^{2-}$

4. Conclusion

In summary, we may conclude that CuIn_3Se_5 was successfully prepared by direct reaction of constituents elements in evacuated silica tube above the melting point. XRD confirmed that CuIn_3Se_5 is formed and crystallizes in the chalcopyrite structure. The transport properties revealed n -type conductivity confirmed by the positive slope in the Mott-Shottky plot. The conductivity is thermally activated and follows an Arrhenius type law.

The compound is thermodynamically stable over the pH range and has been tested successfully for hydrogen generation. The best performance was obtained in $\text{S}_2\text{O}_3^{2-}$ solution (10^{-2} M, pH~7) with an evolution rate of $0.54 \text{ mL g}^{-1} \text{ min}^{-1}$. The present work suggests an attractive way of the solar energy exploitation to convert thiosulfate into hydrogen, a useful energy source.

Acknowledgements

The authors are indebted to M^r S. Omeiri for providing technical assistance.

References

- [1] Barka N, Qourzal S, Assabbane A, Nounah A, Ait-Ichou Y. Factors influencing the photocatalytic degradation of Rhodamine B by TiO_2 -coated non-woven paper. *J Photochem Photobiol A: Chem* 2008;**195**:346-51.
- [2] Omeiri S, Gabe's Y, Bouguelia A, Trari M. Photoelectrochemical characterization of the delafossite CuFeO_2 : application to removal of divalent metals ions. *J Electroanal Chem* 2008;**614**:31-40.
- [3] Roeb M, Neises M, Säck JP, Rietbrock P, Monnerie N, Dersch J. Operational strategy of a two-step thermochemical process for solar hydrogen production. *Int J Hydrogen Energy* 2008;**34**:4537-45.
- [4] Janam R, Rao NN, Srivastava ON. Efficient energy conversion with $n\text{-CuInSe}_2/\text{polysulphide}$ Photoelectrochemical solar cells. *J Phys D: Applied Physics* 1989;**22**:1153-56.
- [5] Djellal L, Omeiri S, Bouguelia A, Trari M. Photoelectrochemical hydrogen-evolution over p -type chalcopyrite CuInSe_2 . *Journal of Alloys and Compounds* 2009;**476**:584–89.
- [6] Djellal L, Bouguelia A, Trari M. Structural, optical and photoelectrochemical properties of CuIn_3Se_5 . *Semicond. Sci. Technol.* 2008;**23**:045019 (7pp).
- [7] Wang H P, Shih I, Champness C H. Studies on monocrystalline CuInSe_2 and CuIn_3Se_5 . *Thin Solid Films* 2000; **361–362**:494-97.
- [8] Malar P, Kasiviswanathan S. Characterization of stepwise flash evaporated CuIn_3Se_5 films. *Sol. Energy Mater. Sol. Cells* 2005;**85**:521-33.
- [9] Bodnar I V, Victorov T, Kushner T L, Rud Yu V. Preparation and photosensitivity investigation of $n\text{-GaSe}/p\text{-CuIn}_3\text{Se}_5$ heterostructures. *Thin Solid Films* 2005; **487**: 199- 201.

- [10] Belhadj M, Tadjer A, Abbar B, Bousahla Z, Bouhafs B, Aourag H. Structural, electronic and optical calculations of Cu(In,Ga)Se₂ ternary chalcopyrites. *Physica Status Solidi (b)* 2004;**241**:2516-28
- [11] Kois J, Bereznev S, Volobujeva O and Mellikov E. Electrochemical etching of copper indium diselenide surface. *Thin Solid Films* 2007;**515**:5871-75